

Estimating Wheat Shoot Nitrogen Content at Vegetative Stage from In Situ Hyperspectral Measurements

Yansong Bao,* Kang Xu, Jinzhong Min, and Jianjun Xu

ABSTRACT

Timely assessment of crop N content is critical for crop growth diagnosis and precision management to generate higher yield and better quality. The objective of this study was to determine the optimal spectral index and build a retrieval model for diagnosing shoot N content (SNC) of wheat (*Triticum aestivum* L.) at vegetative stage using ground-based hyperspectral reflectance data. Hyperspectral indices were investigated to evaluate their capabilities for wheat N concentration estimation by the Pearson's correlation analysis. The analysis results showed that green normalized difference vegetation index (GNDVI) and the combined spectral index the first derivative of reflectance spectral at 736 nm (D736) \times the reflectance at 900 nm (R900)/the reflectance at 720 nm (R720) were most suitable for wheat SNC estimation at vegetative stage. A power model with GNDVI and a linear model with D736 \times R900/R720 were appropriate for SNC estimation in vegetative stage. The validation experiments demonstrated that the power model with GNDVI was preferable to the linear mode with D736 \times R900/R720 for SNC estimation until the flag leaf stage. However, the linear model with D736 \times R900/R720 was better after the flag leaf stage. For wheat SNC assessment at the whole vegetative stage, the linear model with D736 \times R900/R720 was the most accurate, of which the root mean square error was 2.391 g m⁻² and the correlation coefficient between the measured and estimated SNC was 0.934 ($n = 79$).

Key Laboratory of Meteorological Disaster of Ministry of Education, Nanjing Univ. of Information Science and Technology, Nanjing, China, 210044. Received 6 Jan. 2013. *Corresponding author (ysbao@hotmail.com).

Abbreviations: Chl, chlorophyll; D526, the first derivative of reflectance spectral at 526 nm; D736, the first derivative of reflectance spectral at 736 nm; D740, the first derivative of reflectance spectral at 740 nm; DVI, difference vegetation index; GNDVI, green normalized difference vegetation index; LDW, leaf dry weight; LNC, leaf N content; MCARI, modified chlorophyll absorption in reflectance index; NDNI, normalized difference N index; NDSI, normalized difference spectral index; NDVI, normalized difference vegetation index; R720, the reflectance at 720 nm; R860, the reflectance at 860 nm; R900, the reflectance at 900 nm; R990, the reflectance at 990 nm; RMSE, root mean square error; R_{NIR}, the reflectance at near-infrared spectral band; R_{red}, the reflectance at red spectral band; RSI, ratio spectral index; RVI, ratio vegetation index; SDW, stem dry weight; SNC, shoot N content; STNC, stem N content; TAP, total amount of plants; VIOpt, optimal vegetation index.

NITROGEN is an essential nutrient required for plant growth (Kim et al., 2000). Nitrogen uptake determines crop yield and grain quality. An adequate supply of N to crops is fundamental for optimizing yields (Jain et al., 2007). Using less fertilizer may result in the reduction in yields due to N deficiency (Haboudance et al., 2002). However, excessive N supplies can cause surface and ground water contamination (Zhao et al., 2007). Therefore, dynamic fertilization is very important for crop yield and environment protection. For dynamic fertilization, one of the critical technologies is how to determine the N content of crop.

Since most leaf N localized in chlorophyll (Chl) molecules, there is a strong relationship between leaf N and leaf Chl content

Published in Crop Sci. 53:2063–2071 (2013).

doi: 10.2135/cropsci2013.01.0012

Freely available online through the author-supported open-access option.

© Crop Science Society of America | 5585 Guilford Rd., Madison, WI 53711 USA

All rights reserved. No part of this periodical may be reproduced or transmitted in any form or by any means, electronic or mechanical, including photocopying, recording, or any information storage and retrieval system, without permission in writing from the publisher. Permission for printing and for reprinting the material contained herein has been obtained by the publisher.

(Tracy et al., 1992; Han et al., 2001). In near-infrared wavelengths, leaf reflectance is high as a result of low Chl absorption and multiscattering in leaf body. In visible wavelengths, leaf reflectance is relatively low because of high Chl absorption (Curran, 1989). Thus, vegetation reflectance is related with N content. Remote sensing technology can acquire vegetation reflectance; therefore, it could provide inexpensive estimates of N status and be used to monitor N status since leaf Chl *a* content is mainly determined by N availability.

Previous studies have shown that vegetation indices calculated from reflectance data can be successfully used to assess N content of various plants, such as wheat (Filella et al., 1995; Sembiring et al., 1998; Zhao et al., 2012), corn (*Zea mays* L.) (Kim et al., 2000), sweet pepper (*Capsicum annuum* L.) (Thomas and Oerther, 1972), bean (*Phaseolus vulgaris* L.) (Thai et al., 1998), cotton (*Gossypium hirsutum* L.) (Tracy et al., 1992), and rice (*Oryza sativa* L.) (Takebe et al., 1990; Inoue et al., 2012). For example, Wright et al. (2003) used the difference vegetation index (DVI = the reflectance at near-infrared spectral band [R_{NIR}] – the reflectance at red spectral band [R_{red}]) and the ratio vegetation index ($RVI = R_{NIR}/R_{red}$) to retrieve N in grain crop and concluded that DVI obtained the higher r^2 with N, compared to other vegetation indices. Sembiring et al. (1998) used normalized difference vegetation index (NDVI) to predict N uptake for winter wheat and concluded that NDVI was a good index to N uptake. Ranjan

et al. (2012) used green normalized difference vegetation index (GNDVI) to predict leaf N content (LNC). Filella et al. (1995) used three parameters of the red edge to assess total leaf Chl *a* content and concluded that the use of the optical techniques offered a potential for assessing N status of wheat. Some new vegetation indices were also developed to retrieve N, such as normalized difference N index (NDNI) (Serrano et al., 2002), optimal vegetation index (VI_{opt}) (Reyniers et al., 2006), modified chlorophyll absorption in reflectance index (MCARI) (Daughtry et al., 2000), transformed chlorophyll absorption in reflectance index (Haboudance et al., 2002), and normalized ratio indices (Herrmann et al., 2010). Although these vegetation indices were successfully used to predict vegetation N for the specified studies, it is still hard to select a vegetation index that can provide good predictions of crop N content under all circumstances. The main reasons are the performances of vegetation indices depend on the sensor, canopy closure (soil exposed), vegetation characteristics, soil moisture, and environmental effect (Reyniers et al., 2006).

Winter wheat is a main crop in the North China Plain. Timely and accurate estimation of the N content of winter wheat is very important for agricultural management in this region. The focus of this study is to estimate winter wheat shoot N in the North China Plain using remote sensing technology. Various related spectral indices (Table 1) were investigated to assess wheat shoot N

Table 1. Summary of spectral indices studied in this paper.

Spectral indices	Formula [†]	Reference
Normalized ratio index	$NRI_{1510} = (R_{1510} - R_{660}) / (R_{1510} + R_{660})$	Herrmann et al. (2010)
Double-peak canopy N index (DCNI)	$DCNI = (R_{720} - R_{700}) \times (R_{700} - R_{670}) / (R_{720} - R_{670} + 0.03)$	Chen et al. (2010)
Normalized difference N index (NDNI)	$NDNI = [\log(1/R_{1510}) - \log(1/R_{1680})] / [\log(1/R_{1510}) + \log(1/R_{1680})]$	Serrano et al. (2002)
Optimal vegetation index (VI _{opt})	$VI_{opt} = (1 + SAF) \times (R_{800}^2 + 1) / (R_{670} + SAF)$; SAF = 0.45	Reyniers et al. (2006)
Green normalized difference vegetation index (GNDVI)	$GNDVI = (R_{750} - R_{550}) / (R_{750} + R_{550})$	Gitelson et al. (1996)
Normalized difference vegetation index (NDVI)	$NDVI = (R_{800} - R_{670}) / (R_{800} + R_{670})$	Rouse et al. (1974)
Combined index	MCARI/MTVI2: $MCARI = [R_{700} - R_{670} - 0.2(R_{700} - R_{550})] / (R_{700}/R_{670})$ and $MTVI2 = 1.5[1.2(R_{800} - R_{550}) - 2.5(R_{670} - R_{550})] / [(2R_{800} + 1)^2 - [6R_{800} - 5(R_{670})^{1/2}]^{1/2} - 0.5]$	Eitel et al. (2007)
Ratio spectral index (RSI)	$RSI (D740, D522) = D740/D522$	Inoue et al. (2012)
Absorption band depth normalized to the area of the absorption feature (NBD)	$NBD = ABD/A_{Area}$	Liu (2002)
Normalized difference spectral index (NDSI)	$NDSI (R860, R720) = (R860 - R720) / (R860 + R720)$	Yao et al. (2010)
Normalized difference spectral index	$NDSI (D736, D526) = (D736 - D526) / (D736 + D526)$	Yao et al. (2010)
Ratio spectral index	$RSI (R990, R720) = R990/R720$	Yao et al. (2010)
Ratio spectral index	$RSI (D725, D516) = (D725 - D516) / (D725 + D516)$	Yao et al. (2010)
First derivative	$D736 = (R736 - R735) / 1 \text{ nm}$	This study
Combined index	$D736 \times R990/R720$	This study
Combined index	$D736 \times R900/R720$	This study

[†]A_AREA, area of the absorption feature; ABD, absorption band depth; D516, the first derivative of reflectance spectral at 516 nm; D522, the first derivative of reflectance spectral at 522 nm; D526, the first derivative of reflectance spectral at 526 nm; D725, the first derivative of reflectance spectral at 725 nm; D736, the first derivative of reflectance spectral at 736 nm; D740, the first derivative of reflectance spectral at 740 nm; NRI1510, the normalized ratio index at 1510 and 660 nm; MCARI, modified chlorophyll absorption in reflectance index; MTVI2, modified triangular vegetation index; R550, the reflectance at 550 nm; R660, the reflectance at 660 nm; R670, the reflectance at 670 nm; R700, the reflectance at 700 nm; R720, the reflectance at 720 nm; R750, the reflectance at 750 nm; R800, the reflectance at 800 nm; R860, the reflectance at 860 nm; R900, R990, the reflectance at 900 nm; R990, the reflectance at 990 nm; R1510, the reflectance at 1510 nm; R1680, the reflectance at 1680 nm; SAF, soil adjustment factor.

content (SNC). Based on ground-based hyperspectral measurement, the spectral indices were calculated and the statistical analysis between spectral indices and SNC were conducted. The optimal spectral indices were determined for wheat shoot N estimation according to the correlation coefficients. The best-fitting method was used to build the estimation models for SNC estimation. Finally, the models were used to estimate wheat N content based on ground-based hyperspectral reflectance.

MATERIALS AND METHODS

Experimental Setup

The experimental area was located in the suburban counties of Beijing city, China, and belongs to arid and semiarid environments. A total of 27 winter wheat fields were selected from Changping, Shunyi, and Tongxian. The experimental fields were located between 115°58' to 116°50' E long and 39°30' to 40°33' N lat. Each field was a minimum of 4 ha and planted with the same variety of wheat under the same sowing, fertilization, and irrigation procedures. The largest latitudinal distance among these fields was 53 km, and the largest longitudinal distance was 47 km. The study area was flat, and the predominant soil texture was fine clay loam.

Hyperspectral measurement experiments were set up approximately every 15 d during the period from Feekes 4.0 (1 April) to Feekes 11.1 (2 June), which is the critical growing period for winter wheat. Eight ground campaigns were conducted at Feekes 4.0 (1 Apr. 2004), Feekes 4.0 (3 Apr. 2005), Feekes 5.0 (16 Apr. 2004), Feekes 8.0 (21 Apr. 2005), Feekes 10.5.1 (8 May 2005), Feekes 10.5.3 (18 May 2004), Feekes 10.5.4 (22 May 2005), and Feekes 11.1 (2 June 2004) (Zhao et al., 2012).

Data Acquisition

In the central area of each experimental field, wheat canopy spectrum was measured with 25° field of view at a height of 1.3 m under clear blue sky between 1000 and 1400 h in Beijing local time using an ASD FieldSpec Pro spectrometer (Analytical Spectral Devices, Boulder, CO). The spectral ranges were 350 to 2500 nm with a sampling interval of 1.4 nm at 350 to 700 nm and 2 nm at 1050 to 2500 nm (Zhao et al., 2012). Measurements over a 40 by 40 cm BaSO₄ calibration panel were used to calculate wheat canopy reflectance. Vegetation and panel radiance measurements were taken by averaging 20 scans at an interval of 1 s, with a dark current correction at every spectral measurement (Huang et al., 2004). Spectral reflectance was derived as the ratio of reflected radiance to incident radiance estimated by the calibration panel measurement. The saved spectrum file contained continuous spectral reflectance at 1 nm step over the band region of 350 to 2500 nm.

After measuring canopy spectrum at each experiment field, a 0.6 by 0.4 m wheat sample at the spectrum observation location was taken and sealed in a plastic bag. The fresh samples were taken back to laboratory, and then some samples (10 plants per field) were used for N assay and other plants were used to measure dry weight. The total amount of plants (TAP) was counted. Leaves and stems (stems include ears after earing stage) were separated by hand. Those samples for dry weight

measurement were oven dried at 60° until constant weights were reached. Leaf dry weight (LDW) and stem dry weight (SDW) (g) were measured, and LNC and stem N content (STNC) (%) were determined by the Kjeldahl method with a B-339 distillation unit (Zhao et al., 2012). Shoot N content (g m⁻²) was defined as the total amount of N present in the shoot per unit ground area in this study. Shoot N content was calculated as an index of LDW, SDW, LNC, STNC, and sample area as in Eq. [1] (Liu, 2002):

$$\text{SNC} = \{ \text{LDW} \times [\text{TAP}/(\text{TAP} - 10)] \\ \times \text{LNC} + \text{SDW} \times [\text{TAP}/(\text{TAP} - 10)] \\ \times \text{STNC} \} / (0.4 \times 0.6). \quad [1]$$

Correlation Analysis and Nitrogen Retrieval Model

Various spectral indices, which have been evaluated as the optimal vegetation indices for N retrieval in previous studies (Filella et al., 1995; Sembiring et al., 1998; Haboudance et al., 2002; Serrano et al., 2002; Reyniers et al., 2006; Herrmann et al., 2010; Yao et al., 2010; Ranjan et al., 2012; Inoue et al., 2012), were used to analyze the relationship between vegetation indices and wheat SNC. These spectral indices could be classified into four categories: (i) normalized difference indices, which used a few wavebands to reduce the influence of errors or uncertainty due to sensor specification and background differences as well as for enhancing and/or linearizing the spectral response to observed targets (Huete, 1988; Qi et al., 2011), (ii) ratio vegetation indices, which were least influenced by soil bright at leaf area index greater than three (Major et al., 1990), (iii) the first derivative vegetation indices, which could eliminate background signals or noise and enhance weak spectral features (Inoue et al., 2012), and (iv) combined index, which was built by combining normalized difference indices, ratio vegetative indices, and the first derivative vegetation indices. These spectral indices were proved to be more suitable to assess canopy N content, compared to general vegetation indices such as NDVI, structure insensitive pigment index, normalized difference water index, modified soil-adjusted vegetation index (MSAVI), enhanced vegetation index, etc. in previous studies (Filella et al., 1995; Sembiring et al., 1998; Haboudance et al., 2002; Serrano et al., 2002; Reyniers et al., 2006; Herrmann et al., 2010; Yao et al., 2010; Ranjan et al., 2012; Inoue et al., 2012). As discussed in the Results and Discussion section, the reflectance difference at different SNC levels is more apparent at 900 nm than at 990 nm, especially under high SNC condition, and the first derivative of reflectance spectral at 736 nm (D736) is more suitable to assess SNC at high level compared to other wavelengths. Therefore, three new vegetation indices were also used to assess SNC. Their definition is shown in Table 1.

Using the measured hyperspectral data, the spectral indices of the experimental sites were calculated. The Pearson's correlation analyses were conducted between the spectral indices and SNC at each of the eight stages. As N fertilization is conducted mostly at the vegetative stage, the knowledge of SNC at the vegetative stage is more important than at reproductive stage. Therefore, the correlation between shoot N concentration and hyperspectral indices is investigated at the vegetative stage. The data from 1 April to 8 May were applied to assess the

relationship between the spectral indices and SNC at vegetative stage from the erecting to the earing stage. According to the correlation coefficients, the optimal spectral indices were determined to develop empirical models for SNC estimation.

To assess the predictive ability of various spectral indices and methods, curve fitting in least-square method was used to build SNC estimation models at vegetative stage based on the observation data in 2004 and 2005, and the observation data in 2003 (Li et al., 2006) were used to evaluate the estimation models using statistical indicators R and root mean square error (RMSE). In this study, R is the correlation coefficient between the measured and estimated SNC and RMSE is defined as

$$\text{RMSE} = \{[\sum(\hat{y}_i - y_i)^2] / (n - 1)\}^{1/2},$$

in which \hat{y}_i is the predicted values, y_i is the measured values, and n is the amount of observation data (Willimas and Norris, 1987).

Before developing SNC retrieval models, a quality control method was used to select high quality data to build the models. Statistically, if there is a normal distribution of the control values we would have approximately 95% of the points within 2 SD of the mean. This statistical theory was applied to data quality control in this study. The quality control procedure included three steps. First, all data at vegetative stage were used to best fit the SNC retrieval model with the optimal spectral index, and then the model was used to estimate SNC from the optimal spectral indices based on the data at vegetative stage. Second, the differential between measured and retrieved SNC was calculated, and the mean and SD of the differential was also calculated. Third, all data within 2 SD of the mean passed the quality control test and were used to develop the SNC estimation model. The quality control was based on a hypothesis that the optimal spectral indices were able to estimate plant nitrogen content with a high accuracy and a high estimation error might be from a high measurement error. Those data beyond 2 SD of the mean were neglected not to be involved in developing a SNC estimation model.

RESULTS AND DISCUSSION

Optimal Hyperspectral Indices for Nitrogen Retrieval

Figure 1 shows some typical examples of reflectance spectra of wheat canopies with various levels of SNC at the range of 0.555 to 9.087 g m⁻². Four spectral absorption features, centered at 670, 980, 1190, and 1450 nm, and five spectral reflectance features, centered at 560, 900, 1100, 1280, and 1690 nm, were also shown in Fig. 1. The absorption features centered at 670 nm are attributed to Chl absorption (Gitelson et al., 1996). The 980 nm band is related to leaf water absorption (Strachan et al., 2002). Absorption at the 560 nm is associated with the Chl reflection (Gitelson et al., 1996). The 900 nm reflectance feature is generated by leaf structural features (Tarpley et al., 2002). The absorption features of lignin, cellulose, starch, and protein appear near 1690 nm (Curran, 1989). Absorption at the 2230 nm wavelength is associated with oil

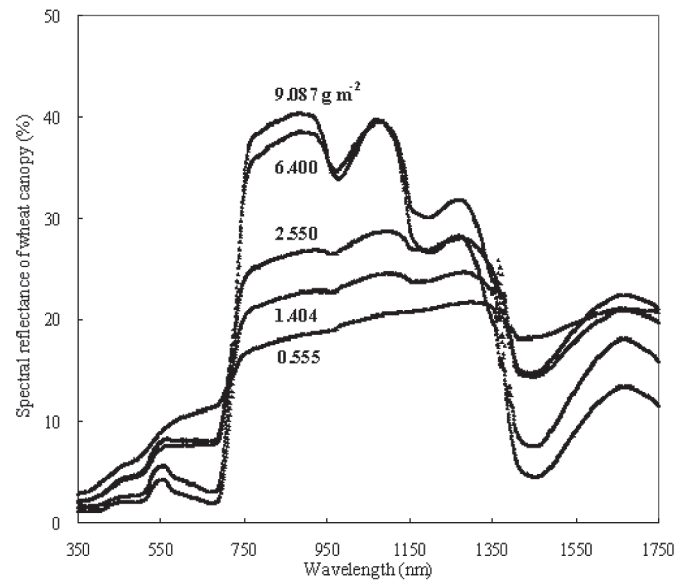


Figure 1. Some typical reflectance spectra of wheat canopies in visible to near-infrared wavelength regions. These spectra are from the ground-based dataset in North China. Numbers indicate the shoot N content (g m⁻²) values.

(Hartwig and Hurburgh, 1990). The spectral regions centered at 1100, 1190, 1280, and 1450 nm were not included in the analysis because they are not commonly used to calculate the spectral index for crop N monitoring. Similar characteristics were also found about rice canopy reflectance (Inoue et al., 2012) whereas the reflectance of wheat canopy was higher than that of rice canopy at early stage. The main reason for the difference is that the reflectance of soil as background is higher than water at the spectral range from visible to near-infrared wavelength region. In canopy reflectance curve, there is a discontinuous segment near 1350 nm as a result of atmosphere impact.

The reflectance curves apparently depicted the responses of canopy spectra to various SNC levels. The reflectance spectra showed a clear positive response to SNC in the near-infrared wavelength region (approximately 760–930 nm) and a negative response in an optical wavelength region (approximately 450–670 nm) and a near-infrared wavelength region (approximately 1400–1530 nm). The positive and negative responses were critical for determining which wavelength reflectance to select to estimate SNC. Since the reflectance features at the range of 760 to 930 nm and 450 to 670 nm are associated with N content, the reflectance in the two ranges would be evaluated to estimate SNC.

Figure 2 shows the first derivative of the reflectance in Fig. 1. As seen at Fig. 2, differences of the first derivative at different SNC levels are most apparent at red edge (670–760 nm). In addition, we found that the red edge position defined as the position of maximal derivative moved approximately from 720 to 736 nm. The similar characteristic was also depicted in a previous study (Liu, 2002).

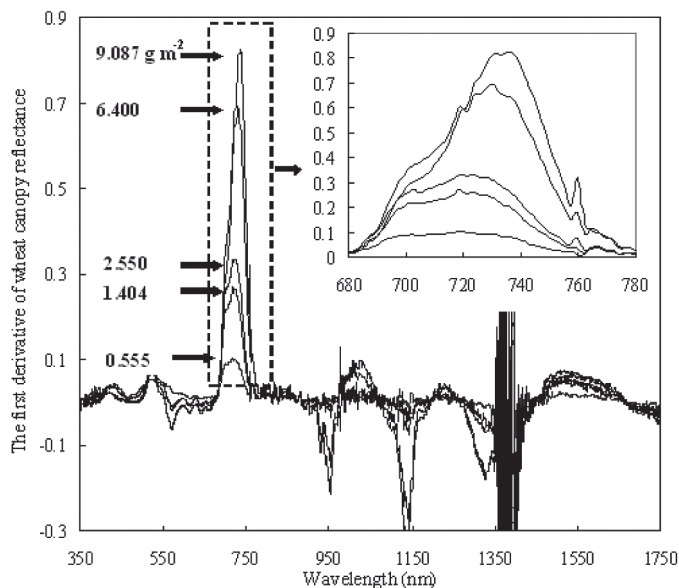


Figure 2. The first derivative of wheat canopy spectral reflectance at 350 to 1750 nm. Numbers indicate the shoot N content (g m^{-2}) values.

Compared to 720 nm, 736 nm is more suitable to be used to assess SNC at high level (Fig. 3). For LNC or canopy N content estimation, high error generally appeared at high N status (Yao et al., 2010); therefore, D736 had the potential to deduce the error of crop N content retrieval.

Table 2 shows the results from Pearson's correlation analysis at the eight growth stages. As seen in Table 2, the hyperspectral indices NDVI, VIopt, the reflectance at 990 nm (R990)/the reflectance at 720 nm (R720), D736 \times the

reflectance at 900 nm (R900)/R720, D736, or normalized difference spectral index (NDSI) (the reflectance at 860 nm [R860], R720) had the highest correlation coefficients with SNC at certain growth stages. Each of NDVI and VIopt had a significant correlation at 0.001 at any one of Feekes 4.0, Feekes 5.0, Feekes 8.0, and Feekes 11.1 and a significant correlation at 0.01 at Feekes 10.5.1. The ratio index R990/R720 obtained a significant correlation at 0.001 at any one of Feekes 4.0, Feekes 5.0, Feekes 8.0, and Feekes 11.1 and a significant correlation at 0.01 at any one of Feekes 10.5.1 and Feekes 10.5.4. Each of D736 and D736 \times R900/R720 obtained a significant correlation at 0.001 at any one of the six stages and a significant correlation at 0.01 at any one of Feekes 10.5.3 and Feekes 10.5.4. The last column of Table 2 shows the correlation coefficients between the spectral indices and SNC at the vegetative stage. As seen at the last column, all spectral indices had significant correlations at 0.001 with SNC. However, the difference of the correlation coefficients was also apparent.

Since the established techniques for the ratio and normalized difference spectral indices could deduce the influence of errors or uncertainty due to sensor specification or atmospheric and background differences (Huete, 1988; Qi et al., 2011; Fernandez et al., 1994; Lyon et al., 1998; Hansen and Schjoerring, 2003; Xue et al., 2004), the spectral indices, such as NDNI, NDSI (D736, the first derivative of reflectance spectral at 526 nm [D526]), NDVI, the normalized ratio index at 1510 and 660 nm [NRI1510], GNDVI, ratio spectral index (RSI) (the first derivative of reflectance spectral at 725 nm [D725], the

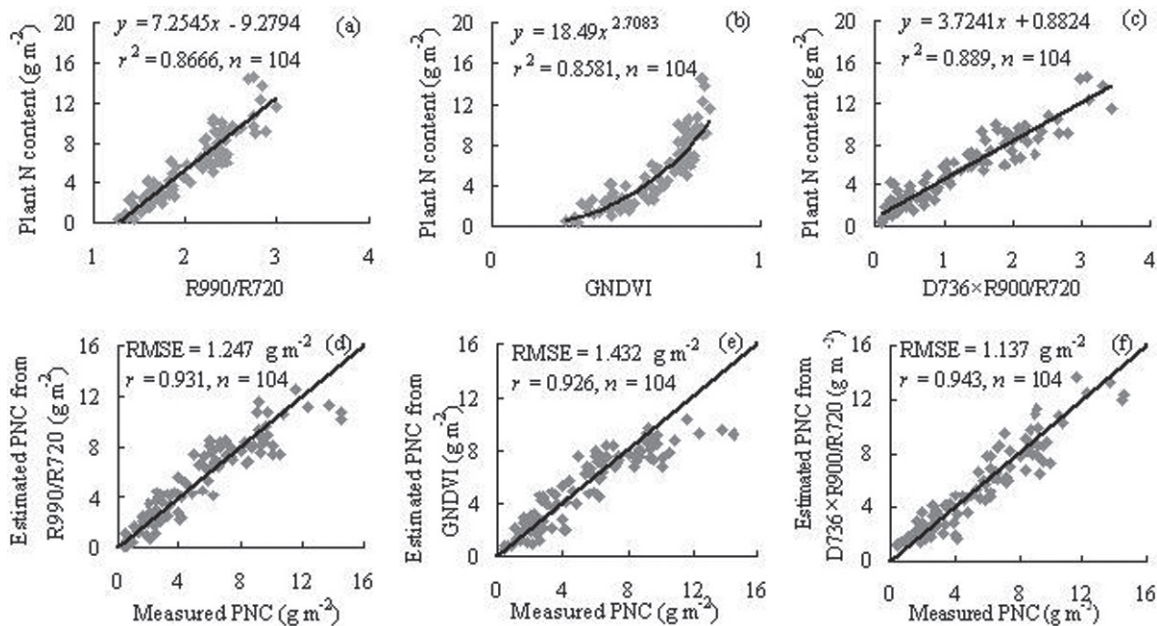


Figure 3. Scatter diagrams and regression lines between shoot N content and the optimal spectral indices [(a) the reflectance at 990 nm [R990]/the reflectance at 720 nm [R720], (b) green normalized difference vegetation index [GNDVI], and (c) the first derivative of reflectance spectral at 736 nm [D736] \times the reflectance at 900 nm (R900)/R720] and scatter diagrams between the measured and estimated shoot N content from R990/R720 (d), GNDVI (e), and D736 \times R900/R720 (f). The 1:1 line is labeled on the plot. PNC, plant nitrogen content; RMSE, root mean square error.

Table 2. Correlation coefficients between hyperspectral indices and shoot N content.†

Experiment date	1 Apr. 2004	3 Apr. 2005	16 Apr. 2004	21 Apr. 2005	8 May 2005	18 May 2004	22 May 2005	2 June 2004	3 Apr.–8 May
Phenophase	Feekes 4.0	Feekes 4.0	Feekes 5.0	Feekes 8.0	Feekes 10.5.1	Feekes 1 0.5.3	Feekes 10.5.4	Feekes 11.1	Vegetative stage
No. of experiment sites	19	25	27	27	14	27	27	27	110
Avg. LAI	1.359	0.572	2.860	2.769	2.863	2.510	2.844	1.428	
NBD	-0.844***	-0.791***	-0.439*	-0.583***	0.077	0.286	0.239	0.243	0.6442***
MCARI/MTVI2	0.261	0.587**	0.505**	0.139	0.320	0.234	0.502**	0.506**	0.6024
DCNI	0.770***	0.864	0.038	0.439*	0.033	0.099	0.203	0.330	0.5540***
NDNI	0.877***	0.845***	0.711***	0.764***	0.566*	0.231	0.320	0.689***	0.8053***
NDSI (D736, D526)	0.802***	0.874***	0.849***	0.805***	0.695**	0.307	0.562**	0.649***	0.8200***
NDVI	0.888***†	0.888***	0.841***	0.801***	0.711**	0.279	0.430*	0.749***	0.8391***
NRI1510	0.787***	0.775***	0.845***	0.823***	0.564*	0.090	0.236	0.452*	0.8572***
GNDVI	0.880***	0.892***	0.872***	0.807***	0.687**	0.308	0.494**	0.738***	0.8638***
Vlopt	0.885***	0.893***	0.844***	0.806***	0.661**	0.465	0.483	0.739***	0.8815***
RSI (D725, D516)	0.851***	0.893***	0.870***	0.800***	0.551*	0.313	0.484*	0.737***	0.8869***
D736	0.843***	0.889***	0.879***	0.834***	0.749**	0.514**	0.547**	0.767***	0.9033***
NDSI (R860, R720)	0.805***	0.774***	0.894***	0.833***	0.722**	0.349	0.631**	0.662***	0.9073***
RSI (D740, D522)	0.853***	0.878***	0.892***	0.806***	0.643**	0.373	0.569**	0.750***	0.9106***
R990/R720	0.878***	0.875***	0.911***	0.828***	0.656**	0.203	0.579**	0.672***	0.9132***
D736 × R990/R720	0.861***	0.884***	0.902***	0.841***	0.772**	0.443*	0.447*	0.723***	0.9188***
D736 × R900/R720	0.859***	0.881***	0.906***	0.843***	0.784***	0.510**	0.573**	0.804***	0.9203***

*Significant at the 0.05 probability level.

**Significant at the 0.01 probability level.

***Significant at the 0.001 probability level.

†LAI, leaf area index; D516, the first derivative of reflectance spectral at 516 nm; D522, the first derivative of reflectance spectral at 522 nm; D526, the first derivative of reflectance spectral at 526 nm; D725, the first derivative of reflectance spectral at 725 nm; D736, the first derivative of reflectance spectral at 736 nm; D740, the first derivative of reflectance spectral at 740 nm; DCNI, double-peak canopy N index; GNDVI, green normalized difference vegetation index; MCARI, modified chlorophyll absorption in reflectance index; MTVI2, modified triangular vegetation index; NBD, absorption band depth normalized to the area of the absorption feature; NDNI, normalized difference N index; NDSI, normalized difference spectral index; NDVI, normalized difference vegetation index; NRI1510, the normalized ratio index at 1510 and 660 nm; R720, the reflectance at 720 nm; R860, the reflectance at 860 nm; R900, R990, the reflectance at 900 nm; R990, the reflectance at 990 nm; RSI, ratio spectral index; Vlopt, optimal vegetation index.

‡The bold and underlined data indicates the highest correlation coefficient at each column.

first derivative of reflectance spectral at 516 nm [D516]), and RSI (the first derivative of reflectance spectral at 740 nm [D740]), the first derivative of reflectance spectral at 522 nm [D522]), obtained high correlation with SNC compared to other spectral indices such as double-peak canopy N index (DCNI), MCARI/modified triangular vegetation index (MTVI2), and absorption band depth normalized to the area of the absorption feature (NBD). In addition, a critical reason for the high correlation coefficients is that these spectral indices used the spectral bands about N content, such as 550 nm (Gitelson et al., 1996), 1510 nm (Herrmann et al., 2010), and red edge (Liu, 2002). Since Vlopt uses red and near-infrared band associated with N content and is a stable vegetation index under circumstances of changing light conditions and platform vibrations (Reyniers et al., 2006), it obtained a high correlation coefficients with SNC.

As seen at last lines in Table 2, those spectral indices have very high correlation coefficients (>0.9) with SNC at vegetative stage. At the same time, we also found that D736 is high correlative with SNC and the ratio index R990/R720 could be used to enhance the response of the first derivative index to SNC. Yao et al. (2010) compared all ratio spectral indices from 350 to 2500 nm and considered

the reflectance ratio between 990 and 720 nm to be the optimal index. Table 2 also shows the RVI R990/R720 obtains high correlation coefficients. However, as seen at Fig. 1, 990 nm is at canopy water absorption band. When canopies were very dense, high canopy water content might deduce the response of R990/R720 to SNC. Nine hundred nanometers was at the peak of near-infrared reflectance (Fig. 1). The reflectance difference at different SNC levels is more apparent at 900 nm than at 990 nm, especially under high SNC condition. Table 2 also shows that wheat SNC is more correlative with D736 × R900/R720 than with D736 × R990/R720.

Evaluating these excellent spectral indices used in previous study, R990/R720 was optimal index for wheat SNC retrieval. Comparing the index D736 × R900/R720 to R990/R720, we found that D736 × R900/R720 had more Pearson's correlation with wheat SNC. The reasons for this result were that D736 and R900 could enhance the ability of hyperspectral data to assess the SNC at high level. This deduction was proved by the correlation coefficients at the last five stages in Table 2. The index D736 × R900/R720 obtained the highest correlation coefficients with SNC almost at the last five stages.

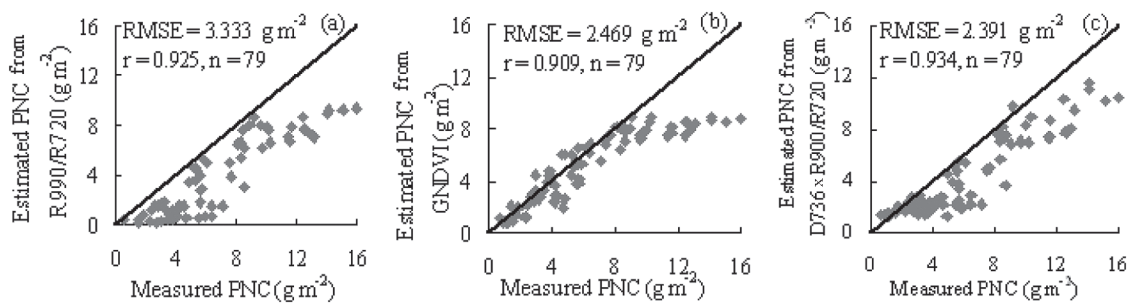


Figure 4. Scatter diagrams between the measured and estimated wheat shoot N content from the linear models with the reflectance at 990 nm (R990)/the reflectance at 720 nm (R720) (a) and the first derivative of reflectance spectral at 736 nm (D736) \times the reflectance at 900 nm (R900)/R720 (b) and the power model (c) with green normalized difference vegetation index (GNDVI). The 1:1 line is labeled on the plot. PNC, plant nitrogen content; RMSE, root mean square error.

The last column of Table 2 shows D736 \times R900/R720 has higher correlation with SNC compared to other vegetation indices. In addition, D736 \times R900/R720 also obtained high correlation coefficients with SNC at each growth stage from 1 April to 8 May. Therefore, D736 \times R900/R720 was selected as the optimal spectral index for SNC estimation in this study. Among these spectral indices, NDSI (D736, D526) and GNDVI could be best fitted by a power function. In addition, the power function with GNDVI got higher determination coefficient R^2 than that with NDSI (D736, D526). Therefore, ability of GNDVI to assess SNC was also investigated. As R990/R720 obtained the highest correlation coefficients with SNC compared to other published spectral indices used in this study, R990/R720 were also evaluated to estimate SNC.

Shoot Nitrogen Concentration Prediction Models and Validation

Figure 3 shows the scatter diagrams between SNC and the three spectral indices (R990/R720, GNDVI, and D736 \times R900/R720) at the vegetative stage. As seen in Fig. 3, R990/R720 and D736 \times R900/R720 have linear relation with SNC (Fig. 3a and 3c); however, the relation between SNC and GNDVI can be best fitted by a power function (Fig. 3b). Therefore, two linear and a power function model were built for SNC retrieval by the least-squares method, using R990/R720, D736 \times R900/R720, and GNDVI, respectively. Figures 3a, 3b, and 3c indicate the three models obtained high determinant coefficients (r^2), and the linear model with D736 \times R900/R720 has the highest r^2 . In addition, Fig. 3d, 3e, and 3f indicate the linear model with D736 \times R900/R720 obtains the smallest RMSE. Therefore, the linear model with D736 \times R900/R720 is optimal model for SNC retrieval at whole vegetative stage. Comparing the linear mode with D736 \times R900/R720 to the power model with GNDVI, it is evident that the linear model overestimates SNC under low N concentration condition ($<1.5 \text{ g m}^{-2}$) and the power model underestimates SNC under high N content condition ($>9.5 \text{ g m}^{-2}$).

To validate the results, the three models were applied in 2003 experiment data at wheat vegetative stage (Li, 2005). These data were acquired on 30 March, 7 April, 15 April, and 1 May in the same experiment region. Figure 4 shows SNC estimation results using the three models. The similar results were found as the results from 2004 to 2005 experiments: (i) the linear model with D736 \times R900/R720 obtained the highest correlation coefficient ($r = 0.934$) and the smallest RMSE (2.391 g m^{-2}) (Fig. 4c); (ii) the linear model with D736 \times R900/R720 overestimated SNC under the low N content condition ($<1.5 \text{ g m}^{-2}$) and underestimated SNC under the high N content condition ($>10 \text{ g m}^{-2}$); however, the accuracy of SNC estimation under the high N content condition is the highest, which is illustrated by the points' nearest approaching the line $y = x$ (Fig. 4c); (iii) the power model underestimated SNC under the high SNC ($>10 \text{ g m}^{-2}$); however, the accuracy of SNC estimation under the N content condition ($<10 \text{ g m}^{-2}$) is the highest, which is also illustrated by the points' nearest approaching the line $y = x$ (Fig. 4b); and (iv) compared to D736 \times R900/R720, R990/R720 acquired a lower accuracy (lower r and bigger RMSE) for SNC estimation (Fig. 4a). As we analyzed in advance, D736 and R900 could enhance the ability of hyperspectral data to assess SNC; therefore, D736 \times R900/R720 provided the most accurate and robust assessment of wheat SNC at vegetative stage, especially under a high N content condition. The critical reason for the excellent performance of GNDVI is using the green band, which was proportional to Chl *a* concentration (Ranjan et al., 2012). Furthermore, the established techniques of GNDVI can deduce the influence of errors due to sensor specification or atmospheric and background differences. However, GNDVI is easy to saturate at high SNC values.

Figure 5 shows the SNC retrieval bias of the experiments sites in 2003. As seen at Fig. 5, the estimation error from the power model with GNDVI is smallest at most experiment sites from 30 March through 15 April; however, the linear model with D736 \times R900/R720 got the smallest estimation error on 1 May. Therefore, the power

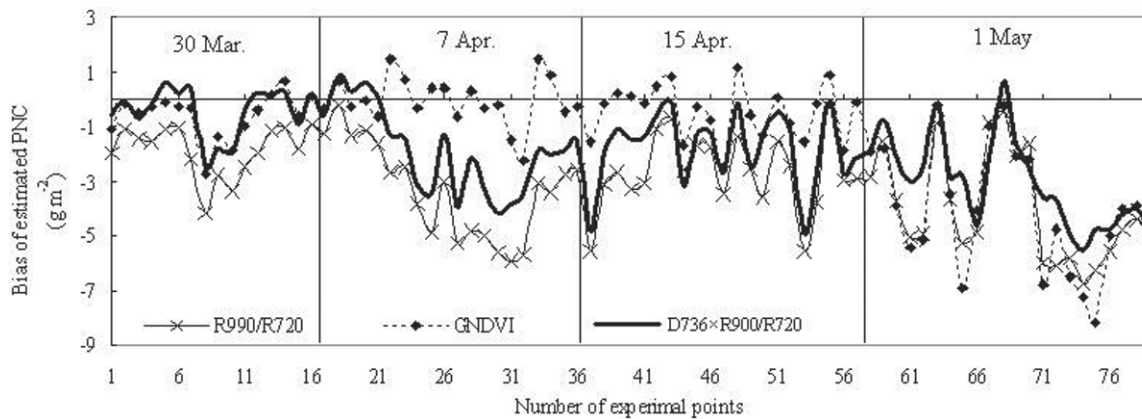


Figure 5. Shoot N content retrieval bias of the experiments sites in 2003. D736, the first derivative of reflectance spectral at 736 nm; R720, the reflectance at 720 nm; R990, the reflectance at 990 nm; GNDVI, green normalized difference vegetation index; PNC, plant nitrogen content.

model with GNDVI is an optimal model for wheat SNC estimation until Feekes 5.0 (around 15 April) whereas the linear model with $D736 \times R900/R720$ is an optimal model for SNC after Feekes 5.0.

DISCUSSION AND CONCLUSIONS

In this study, methods for estimation of wheat SNC were investigated through ground hyperspectral measurements and laboratory experiments. Through statistical analysis of various spectral indices and validation, we found that:

1. Compared to the other hyperspectral indices, GNDVI and $D736 \times R900/R720$ were highly correlated with wheat SNC at most growth stages. In addition, the correlation was higher at the vegetative stage than at the reproductive stage. This result indicated that SNC at vegetative stage could be estimated by hyperspectral measurement method but the N content at reproductive stage could not be estimated with a similar accuracy. For wheat SNC estimation at vegetative stage, GNDVI and $D736 \times R900/R720$ are the optimal hyperspectral indices.
2. The relationship between $D736 \times R900/R720$ and SNC could be depicted by a linear model, and the relationship between GNDVI and SNC could be best fitted by a power model. The power model could acquire a higher accuracy for N content estimation under low and middle N content condition ($<10 \text{ g m}^{-2}$) whereas the linear model could obtain a higher accuracy under high N content condition ($>10 \text{ g m}^{-2}$). Therefore, the two models could be combined to retrieve SNC at vegetative stage. We could use the power model with GNDVI to estimate SNC until Feekes 5.0 and apply the linear model with $D736 \times R900/R720$ to estimate N content after the flag leaf.

Compared to vegetative stage, reproductive stage obtains low correlation coefficients. The main reason could be due to the presence of ears. The combined index $D736 \times R900/R720$ shows higher correlation with wheat plan N content at maturing stage compared to other indices. Therefore, $D736 \times R900/R720$ also has a potential to estimate the yield of wheat.

Acknowledgments

This work was supported by National Natural Science Foundation of China (No.40701130), A Project Funded by the Priority Academic Program Development of Jiangsu Higher Education Institutions (PAPD) and Jiangsu Key Laboratory of Meteorological Observation and Information Processing, Nanjing University of Information Science and Technology, Nanjing, China.

References

- Chen, P., D. Haboudane, N. Tremblay, J. Wang, P. Vigneault, and B. Li. 2010. New spectral indicator assessing the efficiency of crop nitrogen treatment in corn and wheat. *Remote Sens. Environ.* 114:1987–1997. doi:10.1016/j.rse.2010.04.006
- Curran, P.J. 1989. Remote sensing of foliar chemistry. *Remote Sens. Environ.* 30:271–278. doi:10.1016/0034-4257(89)90069-2
- Daughtry, C.S.T., C.L. Walthall, M.S. Kim, E.B. DeColstoun, and J.E. McMurtrey. 2000. Estimating corn leaf chlorophyll concentration from leaf and canopy reflectance. *Remote Sens. Environ.* 74:229–239. doi:10.1016/S0034-4257(00)00113-9
- Eitel, J.U.H., D.S. Long, P.E. Gessler, and A.M.S. Smith. 2007. Using in-situ measurements to evaluate the new Rapid Eye satellite series for prediction of wheat nitrogen status. *Int. J. Remote Sens.* 28:4183–4190. doi:10.1080/01431160701422213
- Fernandez, S., D. Vidal, E. Simon, and L. Sole-Sugranes. 1994. Radiometric characteristics of *Triticum aestivum* cv. Astral under water and nitrogen stress. *Int. J. Remote Sens.* 15:1867–1884. doi:10.1080/01431169408954213
- Filella, I., L. Serrano, J. Serra, and J. Peñuelas. 1995. Evaluating wheat nitrogen status with canopy reflectance indices and discriminant analysis. *Crop Sci.* 35:1400–1405. doi:10.2135/cropsci1995.0011183X003500050023x
- Gitelson, A.A., Y.J. Kaufman, and M.N. Merzlyak. 1996. Use of a green channel in remote sensing global vegetation from EOS-MODIS. *Remote Sens. Environ.* 58:289–298. doi:10.1016/S0034-4257(96)00072-7

- Haboudance, D., J.R. Miller, N. Tremblay, P.J. Zarco-Tejada, and L. Dextraze. 2002. Integrated narrow-band vegetation indices for prediction of crop chlorophyll content for application to precision agriculture. *Remote Sens. Environ.* 81:416–426. doi:10.1016/S0034-4257(02)00018-4
- Han, S., L. Hendrickson, and B. Ni. 2001. Comparison of satellite remote sensing and aerial photography for ability to detect in-season nitrogen stress in corn. An ASAE meeting paper. Paper no. 01-1142. American Society of Agricultural Engineers (ASAE), St. Joseph, MI.
- Hansen, P.M., and J.K. Schjoerring. 2003. Reflectance measurement of canopy biomass and nitrogen status in wheat crops using normalized difference vegetation indices and partial least squares regression. *Remote Sens. Environ.* 86:542–553. doi:10.1016/S0034-4257(03)00131-7
- Hartwig, R.A., and C.R. Hurburgh. 1990. Near-infrared reflectance measurement of moisture, protein and oil content of ground crambe seed. *J. Am. Oil Chem. Soc.* 67:435–437.
- Herrmann, I., A. Karnieli, D.J. Bonfil, Y. Cohen, and V. Alchanatis. 2010. SWIR-based spectral indices for assessing nitrogen content in potato fields. *Int. J. Remote Sens.* 31:5127–5143. doi:10.1080/01431160903283892
- Huang, W., J. Wang, Z. Wang, Z. Jiang, L. Liu, and J. Wang. 2004. Inversion of foliar biochemical parameters at various physiological stages and grain quality indicators of winter wheat with canopy reflectance. *Int. J. Remote Sens.* 25:2409–2419. doi:10.1080/01431160412331269670
- Huete, A.R. 1988. A soil-adjusted vegetation index (SAVI). *Remote Sens. Environ.* 25:295–309. doi:10.1016/0034-4257(88)90106-X
- Inoue, Y., E. Sakaiya, Y. Zhu, and W. Takahashi. 2012. Diagnostic mapping of canopy nitrogen content in rice based on hyperspectral measurements. *Remote Sens. Environ.* 126:210–221. doi:10.1016/j.rse.2012.08.026
- Jain, N., S.S. Ray, J.P. Singh, and S. Panigrahy. 2007. Use of hyperspectral data to assess the effects of different nitrogen applications on a potato crop. *Precis. Agric.* 8:225–239. doi:10.1007/s11119-007-9042-0
- Kim, Y., J.F. Reid, A. Hansen, and M. Dickson. 2000. Evaluation of a multi-spectral imaging system to detect nitrogen stress of corn crops. An ASAE meeting paper. Paper no. 003128. American Society of Agricultural Engineers (ASAE), St. Joseph, MI.
- Li, C. 2005. A research on winter wheat protein monitoring by remote sensing on regional scale. Ph.D. diss., Zhejiang University, Hangzhou, Zhejiang, China.
- Li, Y., Y. Zhu, Y. Tian, X. Yao, X. Qin, and W. Cao. 2006. Quantitative relationship between leaf nitrogen accumulation and canopy reflectance spectra in wheat. *Acta Agron. Sin.* 32:203–209.
- Liu, L. 2002. Hyperspectral remote sensing application in precision agriculture. Post-doctoral research report of Institute of Remote Sensing Applications, Chinese Academy of Sciences, Beijing, China.
- Lyon, J.G., D. Yuan, R.S. Lunetta, and C.D. Elvidge. 1998. A change detection experiment using vegetation indices. *Photogramm. Eng. Remote Sens.* 64:143–150.
- Major, D.J., F. Baret, and G. Guyot. 1990. A ratio vegetation index adjusted for soil brightness. *Int. J. Remote Sens.* 11:727–740. doi:10.1080/01431169008955053
- Qi, J., Y. Inoue, and N. Wiangwang. 2011. Hyperspectral remote sensing in global change studies. In: P.S. Thenkabail, J.G. Lyon, and A. Huete, editors, *Hyperspectral remote sensing of vegetation*. CRC Press, New York, NY. p. 69–90.
- Ranjan, R., U.K. Chopra, R.N. Sahoo, A.K. Singh, and S. Pradhan. 2012. Assessment of plant nitrogen stress in wheat through hyperspectral indices. *Int. J. Remote Sens.* 33:6342–6360. doi:10.1080/01431161.2012.687473
- Reyniers, M., D.J.J. Walvoort, and J.D. Baardemaaker. 2006. A linear model to predict with a multi-spectral radiometer the amount of nitrogen in winter wheat. *Int. J. Remote Sens.* 27:4159–4179. doi:10.1080/01431160600791650
- Rouse, J.W., R.H. Haas Jr., J.A. Schell, D.W. Deering, and J.C. Harlan. 1974. Monitoring the vernal advancement and retrogradation (green wave effect) of natural vegetation. NASA/Goddard Space Flight Center (GSFC) type III final report. NASA/GSFC, Greenbelt, MD.
- Sembiro, H., W.R. Raun, G.V. Johnson, M.L. Stone, J.B. Solie, and S.B. Phillips. 1998. Detection of nitrogen and phosphorus nutrient status in winter wheat using spectral radiance. *J. Plant Nutr.* 21:1207–1233. doi:10.1080/01904169809365478
- Serrano, L., J. Peñuelas, and S.L. Ustin. 2002. Remote sensing of nitrogen and lignin in Mediterranean vegetation from AVIRIS data: Decomposing biochemical from structural signals. *Remote Sens. Environ.* 81:355–364. doi:10.1016/S0034-4257(02)00011-1
- Strachan, I.B., E. Pattey, and J.B. Boisvert. 2002. Impact of nitrogen and environmental conditions on corn as detected by hyperspectral reflectance. *Remote Sens. Environ.* 80:213–224. doi:10.1016/S0034-4257(01)00299-1
- Takebe, M., T. Yoneyama, K. Inada, and T. Murakami. 1990. Spectral reflectance ratio of rice canopy for estimating crop nitrogen status. *Plant Soil* 122:295–297. doi:10.1007/BF02851988
- Tarpley, L.K., R. Reddy, and G.F. Sassenrath-Cole. 2002. Reflectance indices with precision and accuracy in predicting cotton leaf nitrogen concentration. *Crop Sci.* 40:1814–1819. doi:10.2135/cropsci2000.4061814x
- Thai, C.N., M.D. Evans, X. Deng, and A.F. Theisen. 1998. Visible and NIR imaging of bush beans grown under different nitrogen treatments. An ASAE meeting paper. Paper no. 98-3074. American Society of Agricultural Engineers (ASAE), St. Joseph, MI.
- Thomas, J.R., and G.F. Oerther. 1972. Estimating nitrogen content of sweet pepper leaves by reflectance measurements. *Agron. J.* 64:11–13. doi:10.2134/agronj1972.00021962006400010004x
- Tracy, P.W., S.G. Hefner, C.W. Wood, and K.L. Edmisten. 1992. Theory behind the use of instantaneous leaf chlorophyll measurement for determining mid-season cotton nitrogen recommendations. In: *Proceedings of the Beltwide Cotton Conference*, Memphis, TN. 6–10 Jan. 1992. National Cotton Council of America, Memphis, TN. p. 439–443.
- Willimas, P., and K. Norris. 1987. Near-infrared technology in the agricultural and food industries. American Association of Cereal Chemists, St. Paul, MN.
- Wright, D.L., G. Richie, V.P. Rasmussen, R.D. Ramsey, and D. Baker. 2003. Managing grain protein in wheat using remote sensing. Online J. Space Commun. School of Media Arts & Studies at Ohio University, Athens, OH. <http://spacejournal.ohio.edu/pdf/wright.pdf> (accessed 6 June 2012).
- Xue, L., W. Cao, W. Luo, T. Dai, and Y. Zhu. 2004. Monitoring leaf nitrogen status in rice with canopy spectral reflectance. *Agron. J.* 96:135–142. doi:10.2134/agronj2004.0135
- Yao, X., Y. Zhu, Y.C. Tian, W. Feng, and W.X. Cao. 2010. Exploring hyperspectral bands and estimation indices for leaf nitrogen accumulation in wheat. *Int. J. App. Earth Obs. Geoinfo.* 12:89–100. doi:10.1016/j.jag.2009.11.008
- Zhao, B., J. Zhang, M. Flury, A. Zhu, Q. Jiang, and J. Bi. 2007. Ground water contamination with NO₃-N in a wheat-corn cropping system in the north China plain. *Pedosphere* 17:721–731. doi:10.1016/S1002-0160(07)60087-3
- Zhao, C., Z. Wang, J. Wang, and W. Huang. 2012. Relationships of leaf nitrogen concentration and canopy nitrogen density with spectral features parameters and narrow-band spectral indices calculated from field winter wheat spectra. *Int. J. Remote Sens.* 33:3472–3491. doi:10.1080/01431161.2011.604052